SPIRAL GROWTH MANUFACTURING (SGM) – A CONTINUOUS ADDITIVE MANUFACTURING TECHNOLOGY FOR PROCESSING METAL POWDER BY SELECTIVE LASER MELTING.

C. Hauser, C. Sutcliffe, M. Egan and P. Fox.
MSERC, Department of Engineering, University of Liverpool, UK

Abstract

Spiral growth manufacturing is a new innovative powder based rapid manufacturing technique. The innovation exists in the methodology in which powder layers are deposited. Unlike other pre-placed powder systems, the deposited layers move relative to the location at which they are processed. This is made possible by a rotating build drum into which powder is deposited, in spiralled layers, from a stationary hopper. With this configuration powder can be continuously deposited and levelled and simultaneously processed, eliminating delays in the build cycle. Stainless steel and cobalt-chrome powder is selectively melted using a 100W flash lamp pumped Nd:YAG laser. This paper reports on factors affecting build rate and on build strategies for creating a number of axis-symmetric thin and thick walled cylinders. Experimental results suggest that build rate for thin walled structures bonded to a substrate will ultimately be governed by tangential movements of the powder particles when frictional forces are not sufficient to accelerate the particles along a curved path, provided that enough laser power is available for melting. Even melt pool balling, which is evident when melting one layer at high speeds, diminishes in multiple layer builds due to re-melting and infilling.

1. Introduction

Many rapid prototyping (RP) and rapid manufacturing (RM) technologies fundamentally operate as a stop-start process. This occurs because objects are built layer by layer, and each new layer needs preparing and/or moving into position before it can be processed. Hence, layer delivery efficiency influences a large percentage of the overall build speed of many RP systems.

To improve performance a new powder bed variant RM process, Spiral growth manufacturing (SGM), is being developed at Liverpool University which can eliminate delays in the build cycle by allowing simultaneous powder layer delivery and processing. This is made possible with a build platform that revolves and spirals downwards, away from a stationary powder hopper by one layer thickness, for every complete revolution. Hence powder can be continuously deposited and levelled and simultaneously processed at different locations around the build platform. Two machines are currently in development; one uses a bank of stationary inkjet heads to deposit a binding agent into the powder and the other uses a 100W, flash lamp pumped Nd:YAG laser to process metal powder by selective laser melting (SLM). This paper reports on the latter. It has both an application purpose and a fundamental purpose. The application purpose is to seek processing conditions where thin and thick walled parts can be built successfully at speed for application in heat regenerators for Stirling engines. The fundamental purpose is to gain better understanding of the science behind melt behaviour at different scanning conditions when building up layers.

2. Background

2.1 Selective Laser Melting

Selective laser melting (SLM) is an additive manufacturing process in which shaped parts are created from a metal powder bed by fully melting the powder surface layer by layer. SLM evolved from the selective laser sintering (SLS) process as a means to create strong functional parts from familiar materials (titanium, aluminium, tool steels and stainless steels) whilst maintaining the properties of those materials and limiting the need for further operations other than surface finishing [1-3]. Melting occurs using laser or electron beam technology to process the powders by traversing a small spot of heat energy. This, coupled with powder layer delivery, gives comparatively slow build rates (2 to 20mm^3/s) [4]. Good feature resolution and accuracy, high density and near net shape results have been reported for parts produced by SLM [4]. However, these successes are not wide ranging and often component shape is a determining factor; thin walled and honeycombed or lattice structures are easier to construct than solid volumes. There are two main reasons for these difficulties (1) control of flow of molten metal and (2) warping leading to cracking and delamination. Surface tension forces have a large influence on surface flow causing fully molten metal to re-solidify as a series of balls [5-7]. There are a number of approaches to avoiding this. One approach is to avoid full melting. Melt viscosity can be increased if a fraction of the melt remains solid. This is the strategy behind using mixtures of low and high melting point metals [8] and developing alloys with a wide solidus T_S to liquidus T_L melting temperature range [9].

Another approach used to avoid balling is to select laser powers and scan speeds that do not promote instabilities in the melt pool e.g. Rayleigh instabilities [10, 11]. However, this is difficult to control and often results in very narrow process windows. In deep powder beds continuous tracks have been observed from around 1mm/s to 50mm/s [12-13] and continuous single layers have been observed up to 150mm/s [14]. It is reported in [15] that the onset of porosity in melted layers is likely to be analogous to the onset of balling in single tracks. Clearly, there are significant differences in the literature and therefore these systems have not led to reliable commercial SLM technology. Continuous tracks have also been observed in thin powder layers melted to underlying metal substrates. Scan speeds above 100mm/s are reported and this method is now commercialised [16]. Another important aspect of SLM is having enough laser power to melt the current layer and remelt the underlying layer to ensure strong interlayer bonding. This aspect can severely limit the maximum layer thickness that can be processed. Layer thicknesses are typically less than 50μm on commercial machines [16]. This makes the process expensive due to long processing times and the need to use and handle fine powders. As far as warping distortion is concerned, it is not practical to control warping by heating the powder bed to temperatures exceeding half the melting temperature of the alloy; a method employed in plastics SLS. There are methods in which layers can be built up as a collection of patches, to be used with or without substrate support, to distribute and even out the build up of heat over the surface layer. However, commercial technologies all rely on anchoring parts to a rigid substrate. This limits the complexity of parts by restricting the degree of overhang that can be allowed and prevents building geometries that before completion have unconnected features [10].

2.2 Stirling Engine and Heat Regenerators

A Stirling engine (or hot air engine) is a machine which converts heat energy into mechanical work. The function of a Stirling engine is described in detail elsewhere in the literature [17]. It can be used for pumping water, generating electricity or turning industrial machinery. It does not need high quality refined fuels such as petrol or diesel to make it run, but can work on any source of heat, including solar and thermal energy. The Stirling Engine (see Figure 1) relies on the principle that when a quantity of gas is heated (usually air, but sometimes helium or hydrogen), it will expand and its volume will increase. If the gas is sealed in a container, then the pressure inside the container will rise. When cooled, the gas contracts, the volume decreases and thus the pressure will fall. If the container is connected by means of a pipe to a closed power cylinder with an air-tight piston at one end, known as the power piston, on heating the gas pressure will push the piston out (see Figure 1a) until the internal pressure equals atmospheric pressure. With further cooling the internal pressure will fall and the piston will be pushed back in by atmospheric pressure (see Figure 1c) . Once a method is devised to repeatedly heat and cool the gas (usually circulating water for cooling), the piston will reciprocate.

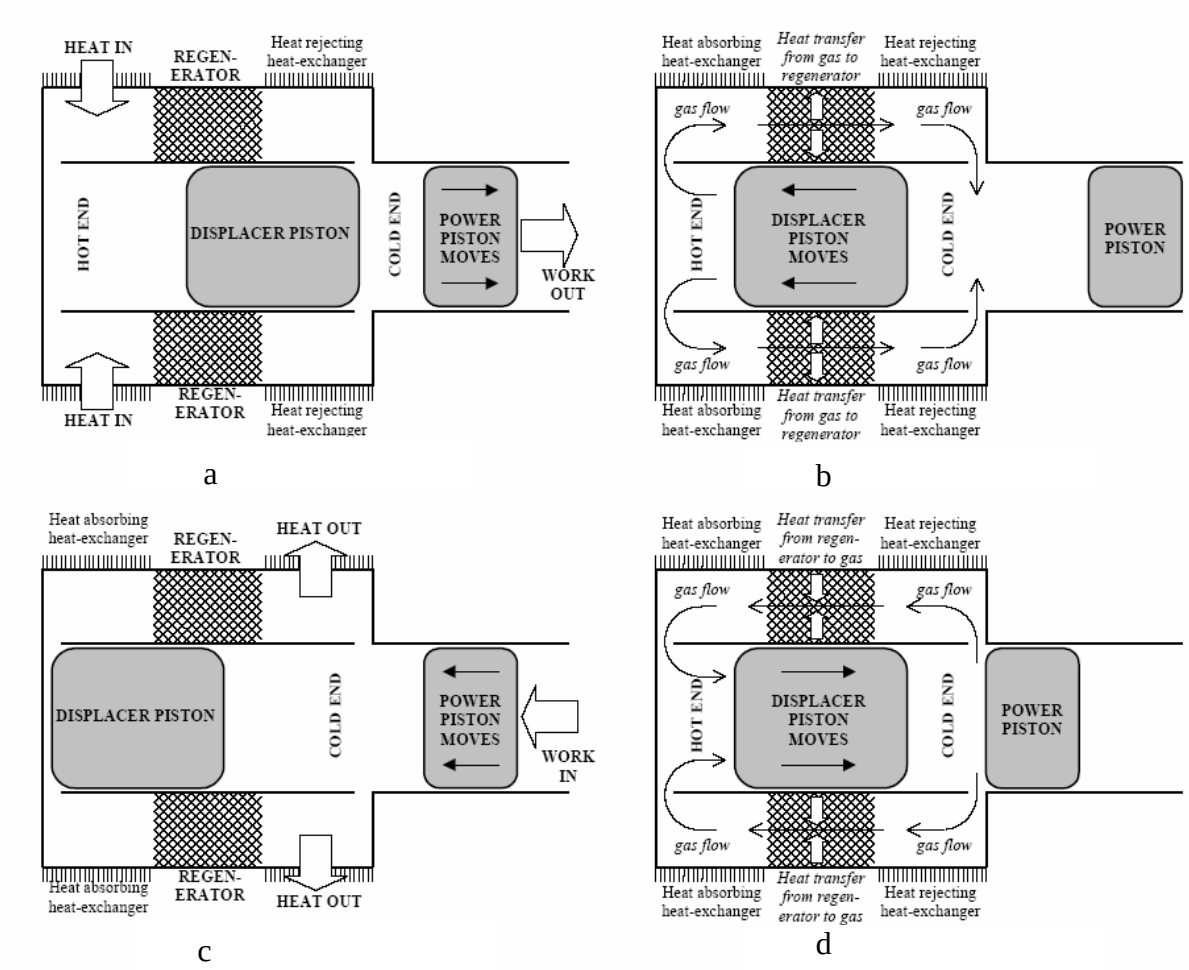

Figure 1: Thermodynamic processes in the ideal Stirling-cycle engine as shown on a simplified β-configuration machine.

In modern Stirling engines a heat store, known as a regenerator, is used to heat and cool the gas. This is situated between the hot and cold ends of the sealed container. Inside the sealed container is a displacer piston which pushes the heated air through the regenerator. The large surface area of the regenerator absorbs heat from the gas, helping to cool it (see Figure 1b). Conversely, the regenerator restores heat to the gas on its return trip to the hot end (see Figure 1d). This reduces the amount of heat which must be put into the system and also means less waste heat needs to be removed, hence increasing efficiency. The regenerator requires a large surface area to provide sufficient thermal contact to the working gas to minimize loss due to irreversible heat transfer while generating as little viscous loss as possible. Historically, regenerators consisted of a mesh or wire wool. However, with modern manufacturing methods, combined with a revival in Stirling engine usage, there is a large research community investigating regenerator design [18,19]. Some example prototype regenerators built at The University of Liverpool by conventional SLM are given in Figure 2. Since a regenerators geometry is often axis-symmetric they are ideally suited for production on an SGM machine.

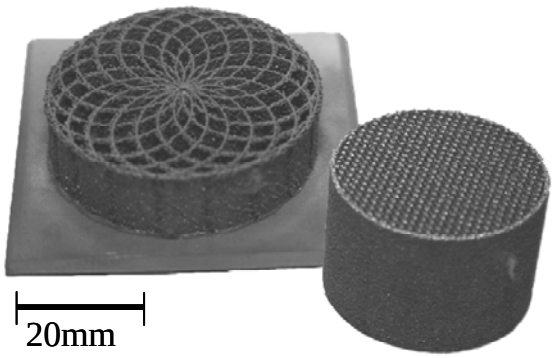

Figure 2: Some example heat regenerators produced at Liverpool University using conventional SLM technology.

3. Experimentation

3.1 Materials.

Gas atomised 316L (0.031C-10.7Ni-16.7Cr-0.34Si-1.71Mn-bal.Fe) stainless steel powder and a cobalt-chrome alloy (80Co, 20Cr) powder has been used in this investigation. The stainless steel powder (particle size range -45μm +10μm) was obtained from Osprey Metals Ltd, UK and the cobalt chrome alloy (particle size range -20 + 50μm) was obtained from Tecphy, France. No heat treatments, additives or fluxes, or powder pre-heating was used in this work. The heat transfer properties of the material for regenerator application are not of concern in this paper.

3.2 SGM Equipment.

An SGM machine, designed and built at the University of Liverpool, was used for all experimental work described in this paper (see Figure 3). Melting was carried out using a 100W flash lamp pumped Nd:YAG laser which was positioned over the SGM apparatus. The spot size

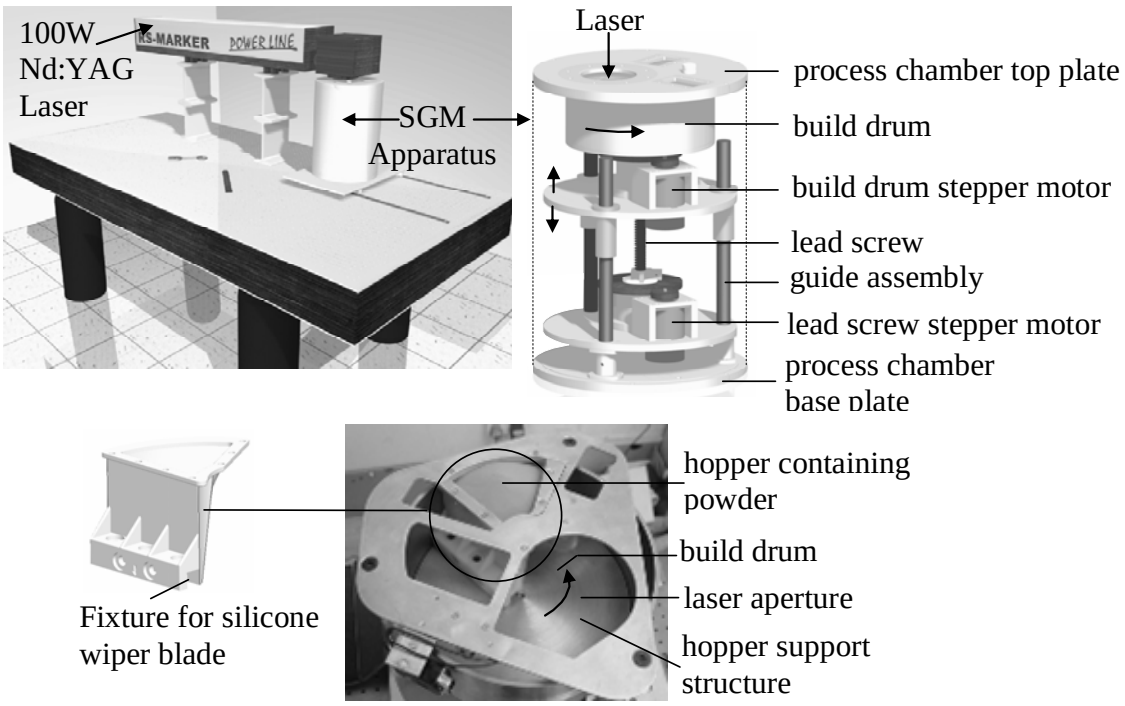

Figure 3: SGM Apparatus

was focused to 0.1mm at the powder bed surface and was scanned by galvanometer driven X-Y scanning mirrors. The laser was run in continuous wave mode. The SGM apparatus was enclosed within a controlled environment process chamber . A window in the chamber roof allowed the beam to enter. Inside the chamber was a 250mm x 60mm deep rotating build drum which could be raised and lowered on a lead screw and guide assembly. Both the drum and lead screw were driven by computer controlled stepper motors. Each motor could be driven independently, for calibration and setup purposes, and could be programmed to run in unison to maintain the required drop (layer thickness) per drum revolution. A stationary hopper, suspended over the drum and supported by extensions at the top of the guide assembly, deposited and spread a continuous spiralled powder layer. A controlled atmosphere reservoir containing additional powder (not shown in Figure 3), which was located outside the process chamber and positioned directly above the hopper, maintained a constant head of powder in the hopper. A sacrificial silicone wiper was fixed to the bottom of the hopper. The hopper was situated 180° circumferentially from the laser processing window. Shielding gas was purged into the main chamber and blown directly over the processing area in the build drum.

The SGM machine can be operated in one of two ways; continuous rotation and processing (see Figure 4a) or intermittent rotation and processing (see Figure 4b). All builds reported in this paper were done using continuous rotation. However, it is important to highlight both build modes since the latter method of rotation allows the laser to scan a stationary powder bed. This will permit more complex geometries to be built with only a predicted small loss in build speed.

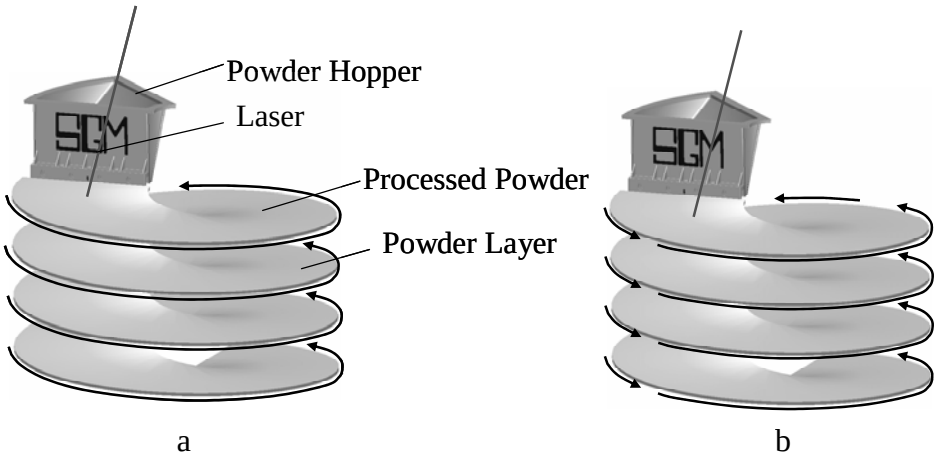

Figure 4: (a) continuous rotation and processing and
(b) intermitted rotation and processing.

3.3 Experimental Conditions.

Thin and thick walled annular rings, with vertical and inclining walls, were created to investigate the feasibility of SGM in producing geometries typically found in heat regenerators. All rings were constructed co-axially with the rotating build drum and had an inner diameter at their base of 50mm and a build height ranging from 6mm up to a maximum of 40mm (limited by volume of powder in the hopper and hopper feeder). Both thin and thick walled rings were produced with spiralled layers with a wall thickness of nominally 1mm and 5mm respectively. The thickness of wall was created by moving the laser at speed (see Table 1), from side to side, perpendicular to the direction of rotation. This had an effect of changing the heating method from a moving point source to a blade of heat which swept over the rotating build drum.

All experiments were carried out in an Argon gas environment (obtained from 99.9% purity bottled argon). The chamber was evacuated to a rough vacuum ($2.5x10^{-3}$mbar) followed by a two minute purge back to atmospheric pressure. This procedure was repeated twice before being followed by a 5 minute pre-melt purge. During processing the flow rate of argon through the chamber was approximately 30 litres/min and the net pressure was kept just above current atmospheric pressure to ensure no air leakage into the chamber. The lamp current was fixed at 20 amps giving 80W of power. All other scanning conditions are reported in Table 1. All builds were bonded to a mild steel substrate which had its bonding surface roughened by grit paper and then cleaned with alcohol prior to its placement in the build drum. On start-up, the laser and drum were operative at the same time. Consequently, half of the substrate was directly irradiated before the deposited powder layer reached the laser beam (due to the opposing locations of the hopper and laser aperture). It should also be highlighted that the layer thickness nominally starts at zero and slowly increases over the first revolution, reaching the specified steady state value under the laser beam after 1.5 revolutions. Finally, part density was calculated from mass and volume data taken from at least three cut sections. Stainless steel 316L was assumed to have a solid density of 7850 kg/m^3.

Table 1: Experimental Conditions.

	Thin Walled		Thick Walled		
Powder	Drum Speed (rpm)	Layer Thickness (μm)	Drum Speed (rpm)	Spiralled Layer Thickness (μm)	Scan speed (mm/s)
316L	5,10,15	45,60,100	10	45	25,50,100, 150,200
Co-Cr	5, 10	45, 60	-	-	-

4. Results and Discussion

4.2 Thin walled annular rings.

Thin walled annular rings were successfully created by melting the stainless steel powder at all conditions set out in section 3.3. Figure 5a illustrates these with a typical example formed at a drum speed of 10rpm and layer thickness of 100μm. All but those rings formed with a 100μm layer thickness and drum speeds of 15rpm appeared, on visual inspection, near to full density. One ring, created at a drum speed of 5rpm and layer thickness of 60μm had a calculated density of 88%. Each build was also strongly bonded to the substrate and could not me removed by hand. This was surprising since during the first 1.5 revolutions of the build drum, the period over which the melt bead was in direct contact with the substrate, balling was observed. The balls were predominantly in single file, tightly packed and estimated to be two or three times greater in diameter than the diameter of the particles in the powder, making the instability difficult to spot on first inspection. Because of the tight packing frequency, particularly at low drum speeds, it was difficult to determine the extent of the instability and whether it was balling or a continuous bead with irregular form being observed. One thing which is clear is that the balls were not to the same scale as those seen when melting deep powder layers [12,15]. As the build height increased the melt bead still formed with some irregularity, but the surface quality of the final part did not reflect on this.

Experiments using the Co-Cr powder were less successful. In each case, the ring became detached from the substrate along almost $^1/_3$ of its circumference, at which point, the walls were also twisted and contracted. This is illustrated in Figure 5b with an example formed at a drum speed of 10rpm and layer thickness of 45μm. It is possible that detachment was caused by poor wetting between the Co-Cr melt and the steel substrate. Evidence to support this comes from the stainless steel results which were successful over the same scanning conditions range.

Partial detachment was most likely caused by the increasing thickness of the first deposited layer (see section 3.3). At the melt pool/substrate interface, the melt pool will refreeze at the point of contact due to the high thermal conductivity of the substrate. When the layer is thicker, the transmitted energy reaching the substrate is lower causing a liquid-solid bond rather than a liquid-liquid bond (no re-melting of the substrate). The strength of a liquid-solid bond is determined by wetting characteristics.

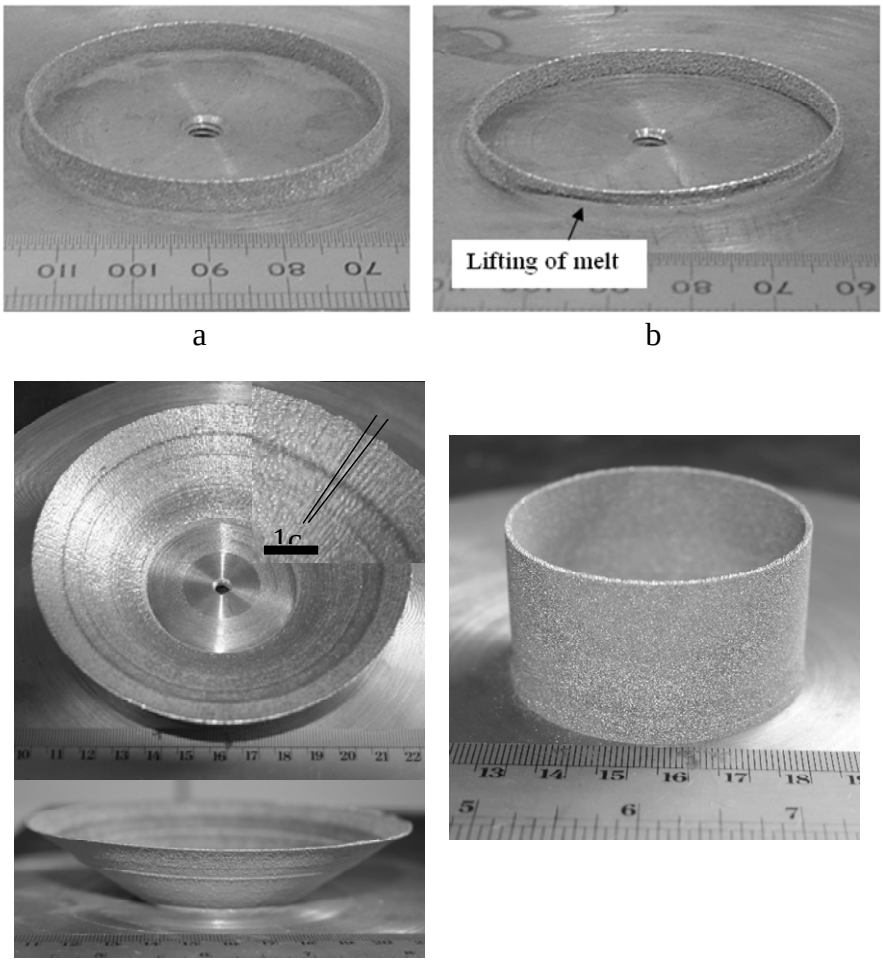

Figure 5: (a) 316L ring formed at 10rpm and 100μm layer thickness, (b) Co-Cr ring formed at 10rpm and 45μm layer thickness, (c) 316L cone formed at 5rpm and 45μm layer thickness and (d) 316L ring formed at 10rpm and 60μm layer thickness.

There are two possible explanations for the shape distortions; (1) melt surface irregularities impede the movement of the build as it passes under the hopper causing layer displacement and (2) temperature variations between layers cause thermal distortions. Since the build is poorly bonded to the substrate there is less resistance to these distortions. Clearly more tests are required on this material. However, the results do highlight the importance of obtaining a strong fusion bond to the underlying substrate.

The time taken to build to a height of 6mm ranged from 4 minutes (calculated using 15rpm and layer thickness of 100μm) to 27 minutes (calculated using 5rpm and layer thickness of 45μm). Over these two extremes the theoretical density of the rings varied from 65% to ~90% respectively; the density varied almost linearly with build time.

Figure 5c/d shows two further build structures, both having greater build heights and one having greater shape complexity (cone). The tests were designed to examine build consistency

over greater processing times. It is important to highlight the surface quality of the cone which had a series of ridges running radially outwards with a high degree of regularity (see Figure 5c). It is suggested that these surface contours are related to the balling phenomenon (see section 5).

4.3 Thick walled annular rings.

Five thick walled annular rings were created by melting stainless steel powder at conditions set out in section 3.3. Figure 6 illustrates these with examples formed at scan speeds of 25mm/s, 50mm/s, 100mm/s and 200mm/s. The build rate, which is governed by drum speed and layer thickness, was constant for all builds. The total build volume for each ring was 5184mm^3 (inner diameter 50mm, wall thickness 5mm and wall height 6mm). The time for each build was 800 seconds (133 layers at 10 layers per minute) giving a build rate of 6.5mm^3/s. The scan speed governed the rate of melting. At low scan speeds (<50mm/s) the laser spot could be considered as a point source of heat traversing, back and forth, across the powder layer perpendicular to the direction of rotation.

At higher speeds the traversing spot merged into a blade of heat that effectively swept over the rotating bed. The two modes of processing caused the powder to melt in different ways. Perhaps some qualitative observations may be relevant here. At low scan speeds the resulting melt bead was well defined, clearly much deeper than the layer thickness and was found to zigzag around the circumference of the annular ring, producing a tight lattice type structure (see Figure 6a/b). The side profile gave a chevron type pattern which, for a scan speed of 50mm/s (see Figure 6b), was notably more porous closer to the substrate. This is perhaps a thermal effect caused by the higher conductivity of the substrate. Porosity occurred exclusively between the melt beads giving an overall average density of approximately 56% for the ring produced at 50mm/s. At high scan speeds there was no defined melt bead, suggesting as expected, a much lower beam intensity. Consequently, the melted surfaces looked similar to that of the loose powder bed, giving a more homogenous structure (see Figure 6c/d). Cracking was also noticeable within the first several layers, around half of the circumference of the ring, causing delamination of the layers. The cracks are likely to be caused by thermal stresses and not through poor wetting since the first one or two layers were still bonded to the substrate. The phenomenon became more pronounced at the higher scan speed suggesting less melting giving weaker interlayer bonds; this would be expected from constant power heating models. Evidence to support this comes from density measurements. Porosity occurred evenly throughout the melt structure giving an overall average density of 53% and 45% for rings produced at 100mm/s and 200mm/s respectively.

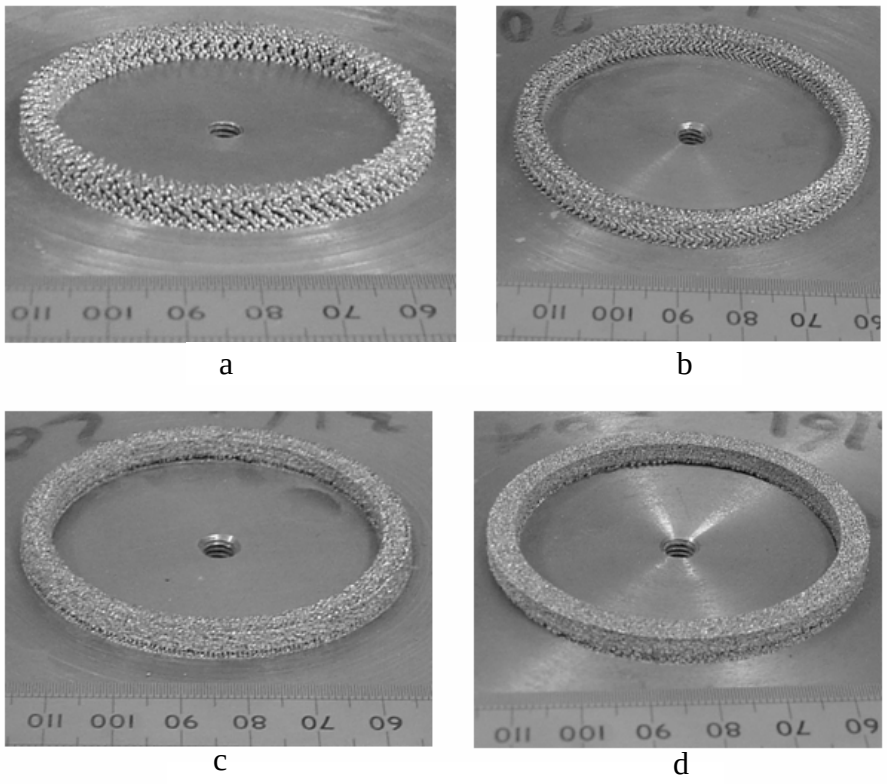

Figure 6: 316L thick walled annular rings formed at 10rpm drum speed, 45μm layer thickness and scan speeds of (a) 25mm/s, (b) 50mm/s, (c) 100mm/s and (d) 200mm/s.

5. Summary and Conclusions

Observations of the formation of thin and thick walled annular rings of two different materials (316L, Co-Cr), with spiralled layer formation are reported. Two methods of scanning were investigated, high and low speed, giving point and blade modes of heating respectively. The low speed scanning gave a marginally higher average build density, greater strength due to the larger localised melt volume and resultant lattice network, but the overall build structure was less homogenous. However, this lattice structure, which is easy and relatively fast to reproduce on the SGM, might be tailored to give congruent channels of porosity which may prove useful in the application of heat regenerators.

Attention was also drawn to the unstable nature of the melt, causing balls to form as the melt front passed over the powder layers surface, particularly at the start when the bead was in contact with the underlying substrate. However, macro scale observations of most of the final parts revealed no obvious evidence of balling or melt instability, suggesting high levels of re-melting of underlying layers and infilling with fresh melt from the surface layer, giving a smoothing effect. One exception to this rule was the top facing surface form of cones with steep angled sides. The surface exhibited a series of ridges running radially outwards around the circumference of the cone. An assumption has been made that this surface form maybe related to

the balling phenomenon since each melted layer does not sit directly on top of the one below, therefore less energy from the laser is available to remelt the underlying layer.

At present build speeds of the SGM range from 5mm^3/s to 8mm^3/s when aiming for part densities greater that 65%, with densities reaching almost 90% at 5mm^3/s (these values were calculated by dividing the melt volume by the time taken to process the part). However, the SGM equipment is not limited by these values. Improvements in scanning strategies may give some increase on the numbers with existing equipment. However, since build rate is determined largely by drum speed and the traverse speed of the laser (and not limited by the layer deposition process) the key to improved speed lies in the lasing equipment and an increase in the amount of power available for melting.

Acknowledgements

This work was carried out at the University of Liverpool as part of a UK EPSRC funded project, ref. no. GR/599013/01. Thanks must be given to Ian Thornton and Keith Thomason for there MSc project work on the development of the spiral slicing algorithm and SGM equipment design respectively. Thanks must also be given to Martin Dunschen and Lawrence Bailey for their invaluable work in writing the SGM control software and building and maintaining the SGM machine respectively.

References

[1] Kruth, J. P. (1991). Material Incress Manufacturing by Rapid Prototyping Techniques, Annals of the CIRP, 40/2:603-614.

[2] Kruth, J. P., Leu, M. C., Nakagawa, T. (1998) Progress in Additive Manufacturing and Rapid Prototyping, Annals of the CIRP, 47/2:525-540.

[3] Kruth, J.P., Mercelis, P. and Van Vaerenbergh, J. (2005). Binding Mechanisms in Selective Laser Sintering and Selective Laser Melting. Rapid Prototyping Journal, 11/1, pp26-36.

[4] Grimm, T. and Sutcliffe, C. (2004). Direct metal technologies focusing on production. Article. Time-compression technologies magazine. Europe Ed. Volume 12, Issues 6.

[5] J.P. Kruth, L. Froyen, J. Van Vaerenbergh, P. Mercelis, M. Rombouts and B. Lauwers, (2004). Selective laser melting of iron-based powder. Journal of Materials Processing Technology149. pp.616-622.

[6] Klocke and C. Wagner (2003). Coalescence behaviour of two metallic particles as base mechanism of selective laser sintering. Annals of the CIRP, 52/1, 177-184.

[7] F. Abe, K. Osakada, M. Shiomi, K. Uematsu and M. Matsumoto (2001). The manufacturing of hard tools from metallic powders be selective laser melting. Journal of Materials Processing Technology, 111, pp.210-213.13.

[8] Zhang, Y., Faghri, A., Buckley, C. W. and Bergman, T. L. Three-dimensional sintering of two-component metal powders with stationary and moving laser beams. Trans. ASME Jnl. of Heat Transfer, 2000, 122, 150-158.14.

[9] Kruth, J. P., Froyen, L., Rombouts, M., Van Vaerenbergh, J. and Mercelis, P. New ferro powder for selective laser sintering of dense parts. Annals of the CIRP, 2003, 52/1, 139-142.

[10] Childs, T. H. C. and Hauser, C. (2005). Selective Laser Sintering (Melting) of Stainless and Tool Steel Powders: Experiments and Modelling. Proc. IMechE Vol. 219 Part B: J. Engineering Manufacturing.

[11] Hauser, C., Childs, T. H. C. and Badrossamay, M. (2004). Further Developments in Process Mapping and Modelling in Direct Metal Selective Laser Melting. In 15th Solid Free Form Fabrication Proceedings, eds. Bourell, R. H. et al., Austin (Texas) August 2-4.

[12] Klocke, F. and Wagner, C. Coalescence behaviour of two metallic particles as base mechanism of selective laser sintering. Annals of the CIRP, 2003, 52/1, 177-184.

[13] Niu, H. J. and Chang, I. T. H. Selective laser sintering of gas atomised M2 high speed steel powder. Jnl. of Materials Science, 2000, 35, 31-38.

[14] Morgan, R., Sutcliffe, C. Papworth, A. and O'Neill, W. (2001). Fabrication of Metal Components by Direct Metal Laser Re-Melting (DMLR). TCT 2001 Proceedings. Rapid News Publications PLC.

[15] Childs, T. H. C. and Hauser, C. (2005). Raster Scan Selective Laser Melting of the Surface Layer of a Tool Steel Powder Bed. Proc. IMechE Vol. 219 Part B: J. Engineering Manufacturing. Pp. 339 - 357

[16] MCP Tooling Technologies. www.mcp-group.co.uk.

[17] West, C.D. (1985). Principles and Applications of Stirling Engines. Van Nostrand Reinhold Company, New York.

[18] Saastamoinen, J .J. (1999). Heat Transfer in Cross Flow Regenerators. International Journal of Heat and Mass Transfer 42. pp. 3205-3216.

[19] Kwanwoo, N. and Sangkwon, J. (2005). Novel Flow Analysis of Regenerator under Oscillating Flow with Pulsating Pressure. Cryogenics 45. pp. 368–379.